Modulation of Redox Potential and Alteration in Reactivity via the Peroxide Shunt Pathway by Mutation of Cytochrome P450 around the Proximal Heme Ligand†

Hirotoshi Matsumura, Masahiro Wakatabi, Sayaka Omi, Akashi Ohtaki, Nobuhumi Nakamura,* Masafumi Yohda, and Hiroyuki Ohno

Department of Biotechnology and Life Science, Tokyo University of Agriculture and Technology, Koganei, Tokyo 184-8588, Japan

Received January 25, 2008; Revised Manuscript Received February 26, 2008

ABSTRACT: In the thermophilic cytochrome P450 from the thermoacidophilic crenarchaeon *Sulfolobus tokodaii* strain 7 (P450st), a phenylalanine residue at position 310 and an alanine residue at position 320 are located close to the heme thiolate ligand, Cys317. Single site-directed mutants F310A and A320Q and double mutant F310A/A320Q have been constructed. All mutant enzymes as well as wild-type (WT) P450st were expressed at high levels. The substitution of F310 with Ala and of A320 with Gln induced shifts in redox potential and blue shifts in Soret absorption of ferrous−CO forms, while spectral characterization showed that in the resting state, the mutants almost retained the structural integrity of the active site. The redox potential of the heme varied as follows: –481 mV (WT), –477 mV (A320Q), –453 mV (F310A), and –450 mV (F310A/A320Q). The trend in the Soret band of the ferrous−CO form was as follows: 450 nm (WT) < 449 nm (A320Q) < 446 nm (F310A) < 444 nm (F310A/A320Q). These results established that the reduction potential and electron density on the heme iron are modulated by the Phe310 and Ala320 residues in P450st. The electron density on the heme decreases in the following order: WT > A320Q > F310A > F310A/A320Q. The electron density on the heme iron infers an essential role in P450 activity. The decrease in electron density interferes with the formation of a high-valent oxo−ferryl species called Compound I. However, steady-state turnover rates of styrene epoxidation with H_2O_2 show the following trend: WT ≈ A320Q < F310A ≈ F310A/A320Q. The shunt pathway which can provide the two electrons and oxygen required for a P450 reaction instead of NAD(P)H and dioxygen can rule out the first and second heme reduction in the catalytic process. Because the electron density on the heme iron might be deeply involved in the k_{cat} values in this system, the intermediate Compound 0 which is the precursor species of Compound I mainly appears to participate dominantly in epoxidation with H_2O_2.

Thermophilic P450 enzymes (*1*) are of interest not only as biocatalysts for chemical synthesis, environmental remediation, and other industrial applications but also in terms of their structural and kinetic analyses (*2, 3*) because they have a high degree of thermotolerance compared with other P450s. Only three cytochrome P450s from thermophiles have been isolated. The melting temperatures for the cytochrome P450 from the thermophilic archaeon *Sulfolobus solfataricus*, CYP119A1, and from the thermophilic bacterium *Thermus thermophilus*, CYP175A1, are 91 and 88 °C, respectively, whereas that for a mesophilic P450cam is approximately 55 °C (*4*−*6*). Cytochrome P450st (P450st)[1] is a soluble thermophilic archaeal enzyme from *Sulfolobus tokodaii* strain 7 (*7*), which exhibits thermal tolerance compared with mesophilic counterparts, as well as other thermophilic P450s, CYP119A1 and CYP175A1.

P450 enzymes are a superfamily of *b* heme-containing monooxygenases, in which a cysteine thiolate acts as the proximal heme ligand (*8*−*10*). They are widespread in all forms of life and have been implicated in numerous biosynthetic and metabolic processes. The P450s are able to catalyze the insertion of an oxygen atom into an inert hydrocarbon with two electrons derived from NAD(P)H via redox partners for activating oxygen molecules. The insertion of an oxygen atom in the reaction process involves the reduction of dioxygen to hydrogen peroxide and the subsequent formation of higher iron oxidation states. The active oxidant species commonly used to perform these reactions is a high-valent oxo−ferryl species called Compound I (Cpd I) (*8*−*11*), which is generated from the precursor species ferric hydroperoxide, so-called Compound 0 (Cpd 0). However, the identity of this species has not been elucidated because of the very fast reaction steps occurring after O_2 binding. Most attempts at trapping Cpd I also led to the oxidative activity of other species in the P450 cycle. Cpd 0 has been implicated as a possible oxidant for several P450 chemistries, which is the last species seen before the product appears in the reaction cycle (*12*−*22*). Notably, the studies

† This study was supported by grants from the Ministry of Education, Science, Sports, Culture, and Technology through the Tokyo University of Agriculture and Technology as a part of the 21st century COE (Center of Excellence) "Future Nano-Materials" Research and Education project, and the Japan Society for the Promotion of Science (Grant 17550149 to N.N.).

* To whom correspondence should be addressed: Department of Biotechnology and Life Science, Tokyo University of Agriculture and Technology, Koganei, Tokyo 184-8588, Japan. Telephone: +81-42-3887482. Fax: +81-42-3887482. E-mail: nobu1@cc.tuat.ac.jp.

[1] Abbreviations: P450st, cytochrome P450 from *S. tokodaii* strain 7; Cpd I, Compound I; Cpd 0, Compound 0; DEAE, diethylaminoethyl; Ni-NTA, nickel-nitrilotriacetic acid; 6cls, a hexacoordinate low-spin.

10.1021/bi800142v CCC: $40.75
Published on Web 03/26/2008

on mutation at the conserved threonine in the proximal heme site suggested that Cpd 0 can play a role in epoxidation. The conserved Thr is very important in the formation of Cpd I with the protonation to dioxygen. The mutants exhibit activity toward double bond epoxidation in spite of the fact that the mutation of Thr could slow or suppress the formation of Cpd I (*14, 18*). Thus, the possible involvement of the Cpd 0 species in oxygenation, including hydroxylation or epoxidation by cytochrome P450, is still controversial, even though the involvement of Cpd I could not be ruled out.

An amino acid sequence comparison of all P450 enzymes reveals that only a few residues are implicitly conserved throughout the superfamily. One of these is the cysteine coordinated to the heme iron (Cys317 in P450st) (*7*). The conservation indicates the importance of the residue. The importance of the Cys residue as the fifth heme ligand in P450 reactions has been demonstrated in theoretical studies and kinetic analyses of model complexes and variant P450s (*23*−*26*). The electron density of the axial cysteine ligand in P450s plays a key role in their unique catalytic activities. The thiolate of the Cys ligand has been proposed to provide a strong electron releasing push effect on the heme iron, which promotes scission of the heterolytic O−O bond to generate Cpd I.

Extensive studies suggest that donation of the electron from the thiolate ligand is controlled by the conserved hydrogen bonds between the thiolate sulfur and surrounding main-chain and side-chain amide NH groups. An earlier mutagenesis-based study of these residues in P450cam missing hydrogen bonds suggested that these hydrogen bonds contribute to the enhanced electronegativity of the thiolate and demonstrated that the enhanced push effect inhibits the protonation of the inner oxygen atom and promotes the protonation of the outer oxygen atom in Cpd 0 (*27, 28*). Consequently, the formation of Cpd I from the precursor Cpd 0 was influenced by the donation of the electron from thiolate, and the donation estimated from its reduction potentials was modulated with the mutation to the residues which exist around the Cys ligand.

In addition, there are several residues placed close to the Cys ligand, which are highly conserved within the "heme-binding" motif. The phenylalanine within the heme-binding loop (Phe393 in P450BM3) is also highly conserved and contributes to the control of the donation of the electron from the thiolate ligand (*29*−*32*). The mutation of Phe393 to Ala, His, Tyr, or Trp affected the electronic environment of the proximal heme ligand, Cys, and modulated the reduction potential of cytochrome P450BM3.

In this study, we initially constructed three mutants and verified whether the mutation of the residues around the ligand affects the redox potential and donation of the electron from thiolate as seen in P450cam and P450BM3. First is the P450st mutant with Phe310 changed to Ala which is at a position similar to that of Phe393 in P450BM3. The second mutation changed Ala320 to Gln, residing close to the conserved cysteine ligand, Cys317 in P450st. The Gln at this position is conserved in the P450 family (Gln360 in P450cam and Gln403 in P450BM3). Third, a double-point mutant, with both F310A and A320Q mutations, was also constructed. These mutants are expected to exhibit a more positive reduction potential than the wild type and suppress the cleavage of the O−O bond of Cpd 0 for the formation of Cpd I. Furthermore, we have experimentally confirmed that Cpd 0 participates in the oxidation of substrates in P450 reactions with the mutants and peroxide shunt pathway. We have employed the shunt pathway which can provide two electrons and an oxygen required for the P450 catalytic cycle instead of electrons from NAD(P)H and dioxygen (*33*−*35*) to rule out the first and second heme reduction in the catalytic process. Hence, it provided evidence for intermediate species in the P450 epoxidation reaction.

EXPERIMENTAL PROCEDURES

Site-Directed Mutagenesis. The preparation of plasmids for the overexpression of wild-type (WT) P450st has been reported previously (*7*). All mutations were engineered into the P450 gene using the standard QuikChange protocol (Stratagene). A full-length P450st gene inserted into the *Nde*I/*Xho*I restriction site of the pET23-b expression vector was used in combination with *Pfu*Turbo DNA polymerase (Stratagene) and the following primer pairs (with the mutation sites underlined): F310A primers, 5′-CCTCATTTGAGTGCCGGTTCTGGAATACA-3′ and 5′-TGTATTCCAGAACCGGCACTCAAATGAGG-3′; A320Q primers, 5′-CATTTATGTTTAGGACAACCTCTAGCGAG-3′ and 5′-CTCGCTAGAGGTTGTCCTAAACATAAATG'3′. Site-specific mutations were confirmed by automated DNA sequencing. Mutants were overexpressed in *Escherichia coli* BL21(DE3) in a manner identical to that of wild-type P450st.

Enzyme Preparations. All cytochrome P450sts (wild-type and mutants) were purified from *E. coli* BL21(DE3) transformants by being grown in 1 L of Luria-Bertani medium containing 100 μg/mL ampicillin and 1 mM δ-aminolevulinic acid at 37 °C without isopropyl β-D-thiogalactopyranoside induction. After an overnight culture, the expressed enzymes were purified as previously described with some modifications (*7*). The *E. coli* cells harboring P450st gene expression plasmids were disrupted by sonication, and the cell lysate was heated at 62 °C to remove *E. coli* proteins. All recombinant P450sts were purified on an anion-exchange diethylaminoethyl (DEAE) column and a nickel-nitrilotriacetic acid (Ni-NTA) affinity column according to the method outlined in our previous paper (*7*). Then, as the final step, the samples were applied onto a Sephacryl S-200 size exclusion column equilibrated in buffer [50 mM Tris-HCl containing 0.2 M NaCl (pH 7.5)].

UV–Vis Absorption Spectroscopy. The electronic absorption spectra were measured at room temperature with a Shimadzu UV-2450 spectrometer. The CO-bound proteins were obtained by the dithionite reduction followed by CO bubbling.

Resonance Raman Spectroscopy. Resonance Raman spectra were recorded on a JASCO NRS-1000 spectrometer using a Kaiser Optical holographic notch-plus filter and a liquid N_2-cooled CCD detector (Princeton Instruments, Spec-10). Raman scattering was excited at 413.1 nm with a Kr ion laser (Coherent, Innova 90C-K), and incident powers were 3.4 mW. The spectra were obtained with data accumulated over 2.5 min and a spectral resolution of 1.47 cm^{-1}. A multiple-point level-fitted fluorescence baseline was performed with GRAMS/386. All measurements were performed at room temperature.

Thermal Stability. The P450st enzymes' activities were assayed at room temperature after preincubation between 25 and 90 °C to investigate the thermostability of the enzymes. P450sts at 1 mg/mL in 50 mM Tris-HCl (pH 7.5) were heated at various temperatures for 30 min. After centrifugation (25000*g* for 30 min), the supernatants were used for the assays.

Steady-State Kinetics. All steady-state kinetic measurements of peroxide-dependent epoxidation assays were performed at 30 °C in 50 mM Tris-HCl buffer at pH 7.5. Reaction mixtures (total volume, 200 μL) contained 20 μM P450st, styrene (40 μM to 1.5 mM), and H_2O_2 (10 mM). Styrene was added as a solution in acetonitrile to give a final acetonitrile concentration of <1.5%. The reaction was initiated by the addition of the enzymes. Control incubations were done without P450st enzymes or without H_2O_2. Samples were then extracted with CH_2Cl_2. The combined CH_2Cl_2 layers were concentrated by evaporation and then analyzed by isothermal gas chromatography (GL-380, GL Science) at 80 °C on a fused silica TC-1 column [30 m × 0.25 mm (inner diameter), GL Science]. Under these conditions, the retention times for styrene and styrene oxide were 2.5 and 5.3 min, respectively. Styrene epoxide formation was quantitated using relative peak areas with acetophenone as the internal standard. The initial P450st concentration was used for all calculations. Assays were performed in triplicate for each substrate concentration, and kinetic constants were calculated with Lineweaver–Burk plots.

Square Wave Voltammetry. To estimate the redox potentials of wild-type P450st and mutants, square wave voltammetry was carried out using an ALS 624B electrochemical analyzer. All square wave voltammetry measurements were performed in 0.1 M phosphate buffer (pH 7.0). A film-coated plastic formed carbon (PFC) electrode was used as a working electrode (working area, 0.071 cm^2). Multilayer films were grown on PFC electrodes. The PFC was polished with water proof abrasive paper (DCC type by Sankyo Rikagaku Co., Ltd., grit number 400) prior to film assembly. The bare PFC electrode was thoroughly washed with water and then sonicated in water for 1 min. Poly(ethyleneimine) (2 mg/mL; average MW of 70000) (PEI) in 0.1 M phosphate buffer (pH 7.0) was used as the polycation for film construction. The (P450st enzyme/PEI) films, where the number of protein−polycation bilayers is 3, were prepared by repeated alternate adsorption for 20 min from a solution of positively charged PEI and negatively charged P450st enzymes. Electrode potentials were measured against a Ag/AgCl (3 M NaCl) electrode with a platinum wire as the counter electrode. Square wave voltammetry conditions were as follows: 2 mV step height, 20 mV pulse height, and 6 Hz frequency. The redox potentials were estimated from the midpoint of reduction−oxidation peaks. All experiments were carried out under an atmosphere of N_2 at room temperature. Square wave voltammetry was performed in triplicate for each sample to average the redox potentials and calculate the experimental errors in each sample.

RESULTS

Overexpression and Purification of P450st Mutants. DNA sequence analysis shows the site-specific mutations introduced into the P450st gene. The F310A, A320Q, and F310A/A320Q variants were successfully overexpressed as a soluble form and subsequently purified to high homogeneity by using a previously described method with some modifications (*7*). All mutant enzymes were expressed at high levels, similar to that of the wild type. The purified enzymes appeared as a single band at a molecular mass of 43 kDa, consistent with the molecular mass deduced from the gene sequences.

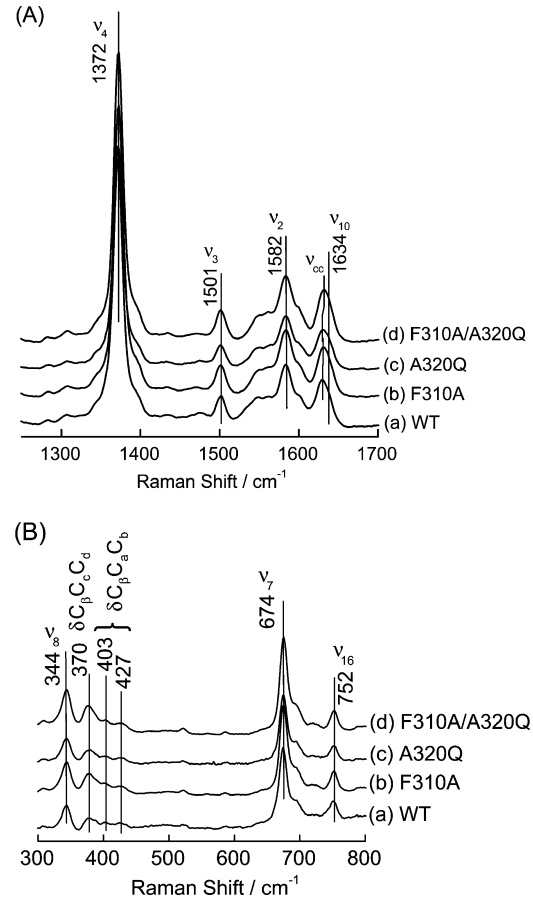

FIGURE 1: Resonance Raman spectra of P450st enzymes in the oxidized form. (A) At high frequencies and (B) low frequencies, Raman spectra of WT P450st (a), F310A (b), A320Q (c), and F310A/A320Q (d) at pH 7.5. All measurements were carried out using excitation at 413.1 nm and incident powers of 3.4 mW at room temperature. All spectra were obtained with data accumulated over 2.5 min and a spectral resolution of 1.47 cm^{-1}.

Spectroscopic Analysis of the Resting State and Carbon Monoxide-Binding P450st Mutants. The purified wild-type and mutant P450sts exhibit a Soret absorbance at 414 nm with a shoulder peak at 360 nm and α and β bands at 532 and 566 nm, respectively, indicating the general feature of cytochrome P450s in a low-spin state. The spectra of the variants were scarcely distinguishable from that of the wild type.

Resonance Raman spectra of WT P450st in its oxidized form using an excitation wavelength of 413.1 nm are shown in Figure 1. At high frequencies (Figure 1A), the Raman bands of wild-type P450st appear at 1372, 1501, 1582, 1629, and 1634 cm^{-1}, indicating a hexacoordinate low-spin (6cls) heme. These frequencies compare well with those reported for another thermophilic P450, CYP119A1 (*4*), and are in good agreement with our reported Raman bands for P450st (*36*). Compared with the spectra of the three mutant enzymes, the differences among the WT, F310A, and A320Q enzymes are small. However, the vinyl stretching vibration, ν_{cc}, which

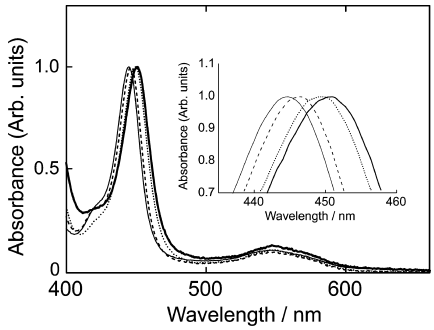

FIGURE 2: UV–vis spectra of the CO-bound ferrous forms of wild-type P450st and F310A, A320Q, and F310A/A320Q mutants. The spectra highlight the deviation in the wavelength of the Soret absorption maximum. The Soret peaks were blue-shifted by 4 nm (F310A, dashed line), 1 nm (A320Q, dotted line), and 6 nm (F310A/A320Q, thin solid line) compared to that of the wild type (thick solid line; $A_{max} = 450$ nm).

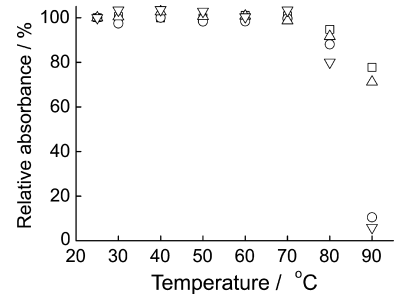

FIGURE 3: Thermal stability of WT and mutant P450st enzymes. The percentage of the residual Soret absorption of WT P450st (□), F310A (○), A320Q (△), and F310A/A320Q (▽) after the incubation at each temperature is represented. The Soret absorption of each sample was normalized by the absorption at 25 °C.

appeared at 1629 cm^{-1} in WT P450st, varies slightly among the mutants. The ν_{cc} vibration at 1629 cm^{-1} can be assigned to an out-of-plane vinyl conformer. The few significant changes in the high-frequency vibrations of WT and mutant enzymes suggest that the heme plane geometry remains almost unchanged. In the low-frequency region as shown in Figure 1B, the ν_{16}, ν_7, and ν_8 modes of wild-type P450st occur at 752, 674, and 344 cm^{-1}, respectively, which also agree with those previously reported (*36*).

Typically, treatment of a reduced Cyt P450s with carbon monoxide generates the characteristic CO−P450 Soret absorption at 450 nm due to the strong donation of an electron from the Cys ligand. The ferrous form of the wild type and all mutant enzymes were capable of generating the Fe^{II}−CO complexes when they were bubbled with CO. While wild-type P450st exhibits a Soret peak at 450 nm as well as spectra typical of CO-bound P450s, blue shifts in the Soret absorption for mutants F310A ($A_{max} = 446$ nm), A320Q ($A_{max} = 449$ nm), and F310A/A320Q ($A_{max} = 444$ nm) were observed (Figure 2). Slight blue shifts were observed, indicating that the substitution of these residues did not lead to an inactive cytochrome P420, the so-called P420 (*37*).

Thermal Stability. The effects of mutations on the thermostability of heme chromophores for wild-type, F310A, A320Q, and F310A/A320Q enzymes were investigated. After preincubation of the enzymes at temperatures between 25 and 90 °C for 30 min, the absorbance maximum of the ferric enzymes at 25 °C was measured. Preincubation for 30 min between 25 and 70 °C did not measurably alter the absorption of the enzymes (Figure 3). While WT P450st and A320Q retained ~80% of the absorption at 25 °C, in F310 mutants, abrupt precipitation occurred when the proteins were preincubated between 80 and 90 °C. The order of thermal tolerance for these enzymes was as follows: WT ≈ A320Q > F310A ≈ F310A/A320Q. The differences in thermostability indicate that the phenylalanine at position 310 in P450st participates in the stabilization of heme groups buried in its protein matrix.

Determination of the Redox Potentials of P450sts. The substrate-free redox potentials of the wild-type, F310A, A320Q, and F310A/A320Q enzymes were measured by square wave voltammetry to verify the effects of the mutations on the redox potential of heme. Figure 4 shows the square wave voltammograms of WT P450st and mutants obtained by the electrostatic layer-by-layer self-assembly technique. Using square wave voltammetry, Figure 4 (wild type) exhibits a peak with a redox potential of Fe^{3+}/Fe^{2+} at –481 mV versus Ag/AgCl (3 M NaCl). A summary of redox potentials for the wild type and mutants determined from a repeated trial is presented in Table 1. The square wave voltammetry gave a redox potential of –481 mV [vs Ag/AgCl (3 M NaCl)] for WT P450st, which is more negative than that with a didodecyldimethylammonium bromide (DDAB) film [−250 mV vs Ag/AgCl (3 M NaCl)] in our previous report (*7*). We have recently studied the characterization of P450st−DDAB films by using UV–vis absorption, resonance Raman spectroscopy, and electrochemical methods (*38*). The results indicated that when working with a P450st−DDAB film, the heme could be released from its protein matrix in DDAB films on PFC electrodes.

Also, the same analysis for P450 mutant enzymes shows that the redox potential of mutants F310A and F310A/A320Q is considerably more positive than that of the wild type [–453 and –450 mV vs Ag/AgCl (3 M NaCl), respectively] and that for the A320Q mutant is rather positively shifted [−477 mV vs Ag/AgCl (3 M NaCl)]. The substitution of phenylalanine at position 310 increased the redox potential of P450st, similar to the mutation of F393 in P450BM3 (*30, 31*).

Kinetics of Styrene Oxidation with Hydrogen Peroxide. No information is available on the endogenous substrates for thermophilic P450st, although sulfur-containing compounds are good candidates for this role given the growth of *S. tokodaii* strain 7 in sulfur-rich environments. After a 30 min incubation of the WT and mutant enzymes with 5 mM styrene and 10 mM H_2O_2, the products were detected by isothermal gas chromatography at 80 °C to confirm the catalytic activity of thermoacidophilic P450sts for styrene and H_2O_2. The sole detectable product detected by gas chromatography was styrene oxide. The styrene oxide was identified by direct chromatographic comparison with an authentic standard. For styrene oxidation, the K_m values varied as follows: F310A/A320Q > A320Q ≈ F310A > WT (as shown in Table 2). The K_m value of each enzyme in this system was large. Because it is difficult to increase the concentration of styrene experimentally, the calculated error bar for each K_m value was large. The observed trend in k_{cat} values was as follows: F310A/A320Q ≈ F310A > A320Q ≈ WT.

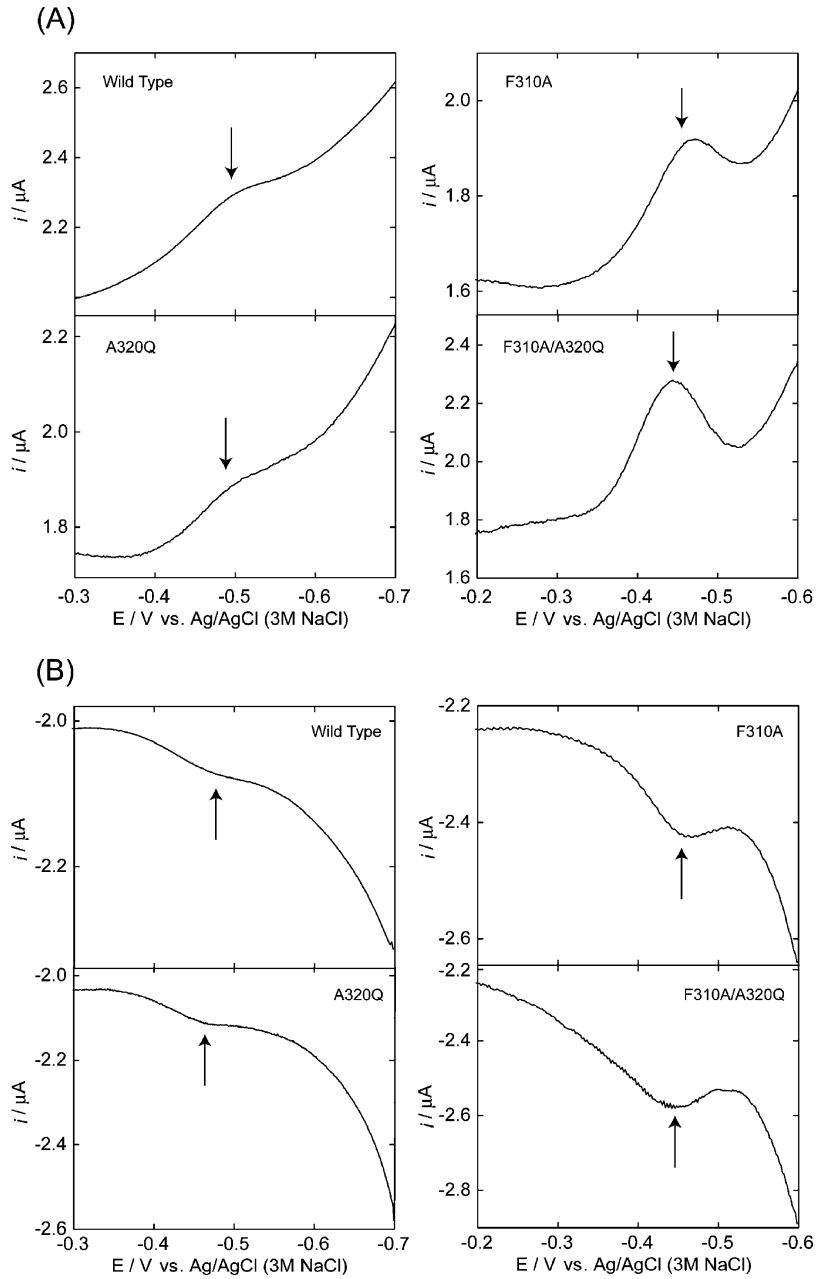

FIGURE 4: Oxidation and reduction square wave voltammetry of PEI−P450st films on a PFC electrode in 0.1 M phosphate buffer at pH 7.0: (A) cathodic scan and (B) anodic scan. Experimental conditions were as follows: square wave amplitude, 20 mV; potential step, 2 mV; frequency, 6 Hz.

Table 1: Redox Potentials for Substrate-Free WT P450st and Mutant P450sts

protein	redox potential [mV vs Ag/AgCl (3 M NaCl)]
wild-type	−481 ± 9
F310A	−453 ± 7
A320Q	−477 ± 9
F310A/A320Q	−450 ± 10

Table 2: Steady-State Kinetics of Styrene Oxidation by the Wild Type and F310A, A320Q, and F310A/A320Q Mutants

protein	K_m ($\times 10^2$ μM)	k_{cat} ($\times 10^{-3}$ s^{-1})
wild-type	1.7 ± 0.9	8.7 ± 0.9
F310A	5.7 ± 1.9	20.8 ± 2.9
A320Q	6.2 ± 2.2	13.3 ± 1.8
F310A/A320Q	8.0 ± 0.9	28.7 ± 2.9

DISCUSSION

Effects of Amino Acid Substitutions at Positions 310 and 320 on Redox Potential. Phenylalanine 310 in P450st is a highly conserved residue throughout the P450 superfamily. Previous mutagenesis studies for P450BM3 indicate that the residue has an influence on electronic nature, reflecting the electron density at the heme iron and heme reduction (*29*−*32*). Glutamine 320 in P450st was conserved in P450cam and P450BM3, which also exists around the thiolate ligand and is involved in controlling reduction potential (*27, 28*). In this study, we constructed P450st mutants with Phe310 changed to Ala and Ala320 to Gln and a double-point mutant with the F310A and A320Q mutations to investigate the effects of these mutations on redox potential and catalytic activity with H_2O_2 (peroxide shunt pathway) (*33*−*35*). Phe310 and

Ala320 in P450st reside close to the conserved cysteine ligand, Cys317, which coordinates with the heme iron.

We successfully expressed and purified the F310A, A320Q, and F310A/A320Q mutants, the yield of which was comparable to that for the WT enzyme. The UV–vis spectral and resonance Raman spectral measurements for the purified mutant enzymes are indicative of a substrate-free low-spin oxidized P450.

The three mutations had little effect on thermostability. On the basis of the homology model (*39*) and the crystal structures of CYP119 and P450st (*5, 7, 40*), three factors have been proposed to contribute to the thermal stability of P450st. The first is a higher density of salt bridges, for example, the Lys49−Asp61−Arg65 salt link in P450st. The second factor is a relatively low density of alanines coupled with a high incidence of isoleucines in the interior of the protein, resulting in better side-chain packing. The third factor is the presence of extended aromatic clusters that are not present in mesophilic P450 structures. One aromatic cluster includes Tyr2, Trp4, Phe5, Phe24, Trp281, and Tyr15. A second cluster is composed of Phe225, Tyr229, Trp231, Phe250, Phe298, Phe334, and Phe338. These observations suggest that the mutation of F310 and A320 hardly has an influence on the overall conformation and thermostability of P450st enzymes. Therefore, all mutants exhibited higher thermal tolerance than the mesophilic counterpart P450cam. However, a difference in thermostability between the F310 mutants (F310A and F310A/A320Q) and the enzymes not mutated at F310 was observed at 90 °C. The difference demonstrates that the interaction of heme groups and phenylalanine at position 310 can be attributed to the thermostability of P450st.

Substitutions of Phe310 and Ala320 of cytochrome P450st have been shown to modulate the redox potential while preserving the structural integrity of the enzyme's active site. The observed trend in redox potential was as follows: F310A/A320Q ≈ F310A > A320Q ≈ WT. The more positive redox potentials of heme iron are totally consistent with the observed blue-shifted Soret band in the ferrous−CO form, suggesting a decrease in the level of backdonation from the thiolate ligand. In the features of CO-bound P450st, differences between the wild type and mutants were observed. The blue shifts indicate a change in the vibrational energy of the CO bond on the heme iron induced by changes in the strength of backbonding from the ferrous heme iron to the CO antibonding orbitals, and hence the electron density at the heme iron (*30*). The blue shift is also indicative of a decrease in electron density at the heme iron because higher electron density increases the degree of backdonation to the CO antibonding orbitals, effectively weakening the CO bond in conjunction with a decrease in the Fe^{II}−CO vibrational energy; thus, absorption would be red-shifted. The blue shifts in the P450st−CO absorption are indicative of an increase in the strength of the CO bond with less backbonding and demonstrate that the order in terms of electron density at the heme iron is as follows: WT > A320Q > F310A > F310A/A320Q. These substitutions of phenylalanine at position 310 and alanine at position 320 with alanine and glutamine, respectively, and both mutations appear to have an influence on the electron density of the heme iron, similar to the nature of these residues in P450cam and P450BM3 (*28, 30*).

Multiple factors are generally considered to influence the redox potential of metalloproteins, for example, the microenvironment and the electrostatic environment around the heme iron (*41*−*45*), the orientation, and the nonplanarity of the heme chromophore (*46*−*48*). The proximal ligand of the redox center as well as the hydrogen bond to the proximal thiolate ligand is also considered to play a key role in modifying redox potential (*25, 26, 49, 50*). Contributions from the heme propionate and vinyl groups (*51*−*54*) have also been considered to be involved in regulating the heme iron redox potential.

Resonance Raman spectroscopy plays a key role in the study of heme proteins because of the strong signal enhancement and detailed vibrational spectrum afforded by the heme group. To obtain detailed insight into the effects of the mutations on the structural formation of the active site, we also measured Soret-enhanced Raman spectra of the oxidized WT and three mutants. Several porphyrin marker bands in the high-frequency region, ν_4, ν_3, ν_2, and ν_{10}, are available for characterizing the heme structure. The band at 1372 cm^{-1} in Raman scattering of wild-type P450st is assigned to the oxidation marker band ν_4, indicating a ferric state of the hemes. Raman bands of WT P450st at 1501, 1582, and 1634 cm^{-1} can be also assigned to heme core vibrations of ν_3, ν_2, and ν_{10}, respectively. The ν_3, ν_2, and ν_{10} frequencies are known as diagnostic markers for the coordination and spin states of the heme (*55*−*59*). The heme core size marker bands ν_3, ν_2, and ν_{10} obtained from the wild-type enzyme are characteristic of a 6cls, analogous to that for the other P450s (*57, 59*). In comparison with the data for F310A, A320Q, and F310A/A320Q mutants, our data show that the mutations do not have a significant effect on the heme core size marker bands.

At low frequencies, the assigned heme skeletal modes in wild-type P450st and mutant enzymes are ν_7 (674 cm^{-1}), ν_8 (344 cm^{-1}), and ν_{16} (752 cm^{-1}). Also, the propionate bending mode $\delta(C_\beta C_c C_d)_{6,7}$ observed at 370 cm^{-1} occurs, indicative of hydrogen bonding of the propionate groups to well-ordered amino acid residues (*60*−*62*). Two vinyl bending modes, $\delta(C_\beta C_a C_b)_{2,4}$, appear at 403 and 427 cm^{-1}, indicating two distinct vinyl conformations (*63*−*65*). According to previous Raman studies of myoglobin (*65*), cytochrome *c* peroxidase (*66*), and P450BM3 (*32*), the frequencies at 403 and 427 cm^{-1} can be assigned to an in-plane vinyl conformer and an out-of-plane vinyl conformer, respectively. Single and double mutations of Phe310 and Ala320 in P450st have a negligible effect on these modes (less than 1 cm^{-1}) at low frequencies, whereas F393 mutants of P450BM3 have changes in those vibrations (*32*).

While changes in the frequencies of the vinyl bending modes were observed in F393 P450BM3 mutants, P450st mutants had no significant change in these frequencies. However, mutations of F310 influence the intensity of the propionate bending mode significantly, consistent with F393 mutants in P450BM3, although an increase in the intensity of A320 mutants was not observed. The detailed mechanism that determines the Raman intensity of the propionate bending mode is not known. However, Chen et al. (*32*) hypothesized that it could relate to the orientation of the propionate groups with respect to the heme plane.

The ν_7 vibration shows that the relative intensities of these modes increase as follows: WT < A320Q < F310A <

F310A/A320Q (which may indicate small differences in heme planarity). However, that there were no significant changes in the high-frequency vibration of WT P450st and its variants suggests that the heme plane geometry remains unchanged. Therefore, the F310 and A320 mutation could induce a change in the protein environment of the vinyl groups. Indeed, investigation of the crystal structure of WT P450st supports the possibility that F310 is in van der Waals contact with the 2-vinyl group as in the crystal structure of P450BM3 (*29*), although a detailed X-ray analysis of these mutants is still underway. Furthermore, considering the studies on P450cam Q360 mutants (*28*), the slight positive shift in the redox potential of A320 mutants with respect to the wild-type enzyme could be attributed to the change in interaction between the heme iron and thiolate ligand via hydrogen bonding, and thus the change in withdrawing the electron density from the heme iron. However, the effects of mutation at position 320 in P450st on electron density may be weaker than that in P450cam because significant frequency shifts were not detected in Raman studies for P450sts and the shift in redox potential was smaller than that for P450cam mutants.

Effects of Amino Acid Substitutions at Positions 310 and 320 on Catalytic Reactions. The monooxidation process catalyzed by cytochrome P450s involves the reduction of dioxygen to hydrogen peroxide followed by the formation of the high-valent oxygen complex species capable of transferring oxygen (*8*−*10*). The reactive species in the cytochrome P450 cycle may be (i) the equivalent of Cpd I of the peroxidases, in which formally the heme iron(IV) state bears an activated oxygen with an oxidizing equivalent on the porphyrin ring ($FeO^{2+}por^{\bullet+}$), or (ii) Cpd 0, the iron(III) bound to a hydroperoxide ($FeOOH^{2+}$). However, the transient character of these intermediates hampers even spectroscopic detection during the reaction cycle under physiological conditions; thus, the reactive intermediates in the P450 reaction cycle are still controversial, and it is still not quite clear to us why only P450 exhibits monooxygenase activity among the heme enzymes in spite of the fact that these enzymes produce Cpd I, as the common oxidant, using either H_2O_2 or O_2, 2 e^-, and 2 H^+. In this study, the catalytic activity for styrene epoxidation with H_2O_2 was assayed using WT P450st and its mutants which have more positive redox potential than the wild type. We have employed styrene as a substrate because the putative product yielded by epoxidation, styrene oxide, is readily analyzed with gas chromatography and there are extensive data on their oxidation by other P450s (*18, 67*). Also, styrene is expected to be a proper substrate for investigating the reactivity of the prospective reactive intermediate Cpd 0, because Cpd 0 could prefer epoxidation to hydroxylation due to its electrophilicity (*18, 22*). Hence, it could be experimentally assessed if an intermediate other than Cpd I catalyzes the oxygenation as the reactive species.

In the comparison among WT P450st and mutant enzymes, the blue shift of the Soret band in the ferrous−CO forms and the change in their redox potential indicate that the electron densities on the heme iron decrease as follows: F310A/A320Q > F310A > A320Q > WT. The electron density on the heme iron, correlated with redox potential, is modulated by multiple contributing factors as mentioned above. Notably, the theoretical calculation using density functional theory and experimental works for P450 mutants and model complexes suggested that the electronic influence of the axial ligand on the heme iron in P450s is the key to their unique reactivities (*8, 10, 23*−*26*). An increase in electron density with more negative reduction potential on the heme iron is believed to result in the promotion of the heterolytic cleavage of heme-bound dioxygen (*27*). Thus, the more positive redox potential shift is expected to interfere with the formation of Cpd I and decrease the rates of styrene oxidation. However, for styrene oxidation, the observed trend in k_{cat} was as follows: F310A/A320Q > F310A > A320Q > WT (which opposes the order for the redox potential among P450st enzymes). The resulting trend for the rate of oxygenation is inconsistent with that for the P450BM3 F393 mutant (*31*).

In the P450BM3 F393 mutant, the higher reduction potentials lowered the catalytic turnover rates, although the stability of the oxy−ferrous complexes and heme reduction rates increased. The catalytic rate-determining step of these P450BM3 enzymes cannot be the initial heme reduction event but is likely to be reduction of the stabilized oxy−ferrous complex and, thereby, the second electron transfer to heme or subsequent protonation. On the other hand, in this study, we have investigated the steady-state kinetics with styrene among P450st variants using a pathway employing H_2O_2 instead of NAD(P)H and the reductases to exclude effects of the second electron transfer to heme. We have used styrene as a test substrate because endogenous substrates for wild-type P450st are still not available, which provide larger K_m values (Table 2). In this study, the formation of the hydroperoxo complex [Fe^{3+}-OOH] species is likely to be the initial step in the reaction of P450st with hydroperoxide. The protonation of the distal oxygen atom bound to the heme iron would be followed by the heterolytic cleavage of the O−O bond to form Cpd I. A study of mutations in P450cam suggested that the decrease in electron density on the heme iron could disturb the protonation to the outer oxygen atom (*27*). Therefore, in the reaction of these P450st mutants bearing more positive redox potentials, the formation of Cpd I could be prevented. We concluded that intermediates such as Cpd 0 mainly participate in the styrene epoxidation, although the formation of Cpd I cannot be ruled out completely.

In summary, our single and double site-directed mutations of F310 and A320 in P450st have revealed that the intermediate Cpd 0 mainly catalyzes the styrene epoxidation with H_2O_2. We have constructed mutants F310A, A320Q, and F310A/A320Q in which the phenylalanine at position 310 and the alanine at position 320 are in the vicinity of the thiolate ligand to the heme. The mutation at position 310 influenced the electron density and reduction potential on the heme iron. We have also used H_2O_2 to rule out the first and second heme reduction in the catalytic process and assess if the intermediate Cpd 0 participates in P450 activity and employed styrene as a test substrate for epoxidation since Cpd 0 may have electrophilic properties. Our results showed that the steady-state turnover rate of styrene epoxidation was greater with the increase in the redox potential of the heme despite the prediction that an increase in redox potential interferes with the formation of Cpd I. Hence, in this case, we postulate that the intermediate Cpd 0 instead of Cpd I

mainly catalyzes styrene epoxidation with H_2O_2 as an electrophilic oxidant.

REFERENCES

1. Nishida, C. R., and Ortiz de Montellano, P. R. (2005) Thermophilic cytochrome P450 enzymes. *Biochem. Biophys. Res. Commun. 338*, 437–445.
2. Kellner, D. G., Hung, S.-C., Weiss, K. E., and Sligar, S. G. (2002) Kinetic characterization of Compound I formation in the thermostable cytochrome P450 CYP119. *J. Biol. Chem. 277*, 9641–9644.
3. Newcomb, M., Zhang, R., Chandrasena, R. E. P., Halgrimson, J. A., Horner, J. H., Makris, T. M., and Sligar, S. G. (2006) Cytochrome P450 Compound I. *J. Am. Chem. Soc. 128*, 4580–4581.
4. Koo, L. S., Tschirret-Guth, R. A., Straub, W. E., Moënne-Loccoz, P., Loehr, T. M., and Ortiz de Montellano, P. R. (2000) The active site of the thermophilic CYP119 from *Sulfolobus solfataricus*. *J. Biol. Chem. 275*, 14112–14123.
5. Yano, J. K., Koo, L. S., Schuller, D. J., Li, H., Ortiz de Montellano, P. R., and Poulos, T. L. (2000) Crystal structure of a thermophilic cytochrome P450 from the archaeon *Sulfolobus solfataricus*. *J. Biol. Chem. 275*, 31086–31092.
6. Yano, J. K., Blasco, F., Li, H., Schmid, R. D., Henne, A., and Poulos, T. L. (2003) Preliminary characterization and crystal structure of a thermostable cytochrome P450 from *Thermus thermophilus*. *J. Biol. Chem. 278*, 608–616.
7. Oku, Y., Ohtaki, A., Kamitori, S., Nakamura, N., Yohda, M., Ohno, H., and Kawarabayasi, Y. (2004) Structure and direct electrochemistry of cytochrome P450 from the thermoacidophilic crenarchaeon, *Sulfolobus tokodaii* strain. *J. Inorg. Biochem. 98*, 1194–1199.
8. Ortiz de Montellano, P. R. (2005) *Cytochrome P450: Structure, Mechanism, and Biochemistry*, 3rd ed., Kluwer Academic/Plenum Publishers, New York.
9. Denisov, I. G., Makris, T. M., Sligar, S. G., and Schlichting, I. (2005) Structure and chemistry of cytochrome P450. *Chem. Rev. 105*, 2253–2277.
10. Shaik, S., Kumar, D., de Visser, S. P., Altun, A., and Thiel, W. (2005) Theoretical perspective on the structure and mechanism of cytochrome P450 enzymes. *Chem. Rev. 105*, 2279–2328.
11. Harris, D. L. (2001) High-valent intermediates of heme proteins and model compounds. *Curr. Opin. Chem. Biol. 5*, 724–735.
12. Newcomb, M., Le Tadic-Biadatti, M.-H., Chestney, D. L., Roberts, E. S., and Hollenberg, P. F. (1995) A nonsynchronous concerted mechanism for cytochrome P-450 catalyzed hydroxylation. *J. Am. Chem. Soc. 117*, 12085–12091.
13. Pratt, J. M., Ridd, T. I., and King, L. J. (1995) Activation of H_2O_2 by P450: Evidence that the hydroxylating intermediate is iron(III)-coordinated H_2O_2 and not the ferryl FeO^{3+} complex. *J. Chem. Soc., Chem. Commun.,* 2297–2298.
14. Vaz, A. D. N., McGinnity, D. F., and Coon, M. J. (1998) Epoxidation of olefins by cytochrome P450: Evidence from site-specific mutagenesis for hydroperoxo-iron as an electrophilic oxidant. *Proc. Natl. Acad. Sci. U.S.A. 95*, 3555–3560.
15. Davydov, R., Makris, T. M., Kofman, V., Werst, D. E., Sligar, S. G., and Hoffman, B. M. (2001) Hydroxylation of camphor by reduced oxy-cytochrome P450cam: Mechanistic implications of EPR and ENDOR studies of catalytic intermediates in native and mutant enzymes. *J. Am. Chem. Soc. 123*, 1403–1415.
16. Volz, T. J., Rock, D. A., and Jones, J. P. (2002) Evidence for two different active oxygen species in cytochrome P450 BM3 mediated sulfoxidation and N-dealkylation reactions. *J. Am. Chem. Soc. 124*, 9724–9725.
17. Hutzler, J. M., Powers, F. J., Wynalda, M. A., and Wienkers, L. C. (2003) Effect of carbonate anion on cytochrome P450 2D6-mediated metabolism in vitro: The potential role of multiple oxygenating species. *Arch. Biochem. Biophys. 417*, 165–175.
18. Jin, S., Makris, T. M., Bryson, T. A., Sligar, S. G., and Dawson, J. H. (2003) Epoxidation of olefins by hydroperoxo-ferric cytochrome P450. *J. Am. Chem. Soc. 125*, 3406–3407.
19. Chandrasena, R. E. P., Vatsis, K. P., Coon, M. J., Hollenberg, P. F., and Newcomb, M. (2004) Hydroxylation by the hydroperoxy-iron species in cytochrome P450 enzymes. *J. Am. Chem. Soc. 126*, 115–126.
20. Derat, E., Kumar, D., Hirao, H., and Shaik, S. (2006) Gauging the relative oxidative powers of Compound I, ferric-hydroperoxide, and the ferric-hydrogen peroxide species of cytochrome P450 toward C-H hydroxylation of a radical clock substrate. *J. Am. Chem. Soc. 128*, 473–484.
21. Hirao, H., Kumar, D., and Shaik, S. (2006) On the identity and reactivity patterns of the "second oxidant" of the T252A mutant of cytochrome $P450_{cam}$ in the oxidation of 5-methylenenylcamphor. *J. Inorg. Biochem. 100*, 2054–2068.
22. Koppenol, W. H. (2007) Oxygen activation by cytochrome P450: A thermodynamic analysis. *J. Am. Chem. Soc. 129*, 9686–9690.
23. Dawson, J. H., Holm, R. H., Trudell, J. R., Barth, G., Linder, R. E., Bunnenberg, E., Djerassi, C., and Tang, S. C. (1976) Magnetic circular dichroism studies. 43. Oxidized cytochrome P-450. Magnetic circular dichroism evidence for thiolate ligation in the substrate-bound form. Implications for the catalytic mechanism. *J. Am. Chem. Soc. 98*, 3707–3709.
24. Dawson, J. H. (1988) Probing structure-function relations in heme-containing oxygenases and peroxidases. *Science 240*, 433–439.
25. Auclair, K., Moënne-Loccoz, P., and Ortiz de Montellano, P. R. (2001) Roles of the proximal heme thiolate ligand in cytochrome $P450_{cam}$. *J. Am. Chem. Soc. 123*, 4877–4885.
26. Yoshioka, S., Takahashi, S., Hori, H., Ishimori, K., and Morishima, I. (2001) Proximal cysteine residue is essential for the enzymatic activities of cytochrome $P450_{cam}$. *Eur. J. Biochem. 268*, 252–259.
27. Yoshioka, S., Takahashi, S., Ishimori, K., and Morishima, I. (2000) Roles of the axial push effect in cytochrome P450cam studied with the site-directed mutagenesis at the heme proximal site. *J. Inorg. Biochem. 81*, 141–151.
28. Yoshioka, S., Tosha, T., Takahashi, S., Ishimori, K., Hori, H., and Morishima, I. (2002) Roles of the proximal hydrogen bonding network in cytochrome P450cam-catalyzed oxygenation. *J. Am. Chem. Soc. 124*, 14571–14579.
29. Ost, T. W. B., Munro, A. W., Mowat, C. G., Taylor, P. R., Pesseguiero, A., Fulco, A. J., Cho, A. K., Cheesman, M. A., Walkinshaw, M. D., and Chapman, S. K. (2001) Structural and spectroscopic analysis of the F393H mutant of flavocytochrome P450 BM3. *Biochemistry 40*, 13430–13438.
30. Ost, T. W. B., Miles, C. S., Munro, A. W., Murdoch, J., Reid, G. A., and Chapman, S. K. (2001) Phenylalanine 393 exerts thermodynamic control over the heme of flavocytochrome P450 BM3. *Biochemistry 40*, 13421–13429.
31. Ost, T. W. B., Clark, J., Mowat, C. G., Miles, C. S., Walkinshaw, M. D., Reid, G. A., Chapman, S. K., and Daff, S. (2003) Oxygen activation and electron transfer in flavocytochrome P450 BM3. *J. Am. Chem. Soc. 125*, 15010–15020.
32. Chen, Z., Ost, T. W. B., and Schelvis, J. P. M. (2004) Phe393 mutants of cytochrome P450 BM3 with modified heme redox potentials have altered heme vinyl and propionate conformations. *Biochemistry 43*, 1798–1808.
33. Hrycay, E. G., Gustafsson, J.-å., Ingelman-Sundberg, M., and Ernster, L. (1975) Sodium periodate, sodium chlorite, organic hydroperoxides, and H_2O_2 as hydroxylating agents in steroid hydroxylation reactions catalyzed by partially purified cytochrome P-450. *Biochem. Biophys. Res. Commun. 66*, 209–216.
34. Lichtenberger, F., Nastainczyk, W., and Ullrich, V. (1976) Cytochrome P450 as an oxene transferase. *Biochem. Biophys. Res. Commun. 70*, 939–946.
35. Nordblom, G. D., White, R. E., and Coon, M. J. (1976) Studies on hydroperoxide-dependent substrate hydroxylation by purified liver microsomal cytochrome *P*-450. *Arch. Biochem. Biophys. 175*, 524–533.
36. Matsumura, H., Wiwatchaiwong, S., Nakamura, N., Yohda, M., and Ohno, H. (2006) A novel method for direct electrochemistry of a thermoacidophilic cytochrome P450. *Electrochem. Commun. 8*, 1245–1249.
37. Omura, T., and Sato, R. (1964) The carbon monoxide-binding pigment of liver microsomes. I. Evidence for its hemoprotein nature. *J. Biol. Chem. 239*, 2370–2378.
38. Wiwatchaiwong, S., Matsumura, H., Nakamura, N., Yohda, M., and Ohno, H. (2007) Spectroscopic and electrochemical characterization of cytochrome P450st-DDAB films on a plastic-formed carbon electrode. *Electroanalysis 19*, 561–565.
39. Chang, Y.-T., and Loew, G. (2000) Homology modeling, molecular dynamics simulations, and analysis of CYP119, a P450 enzyme from extreme acidothermophilic archaeon *Sulfolobus solfataricus*. *Biochemistry 39*, 2484–2498.
40. Park, S.-Y., Yamane, K., Adachi, S., Shiro, Y., Weiss, K. E., Maves, S. A., and Sligar, S. G. (2002) Thermophilic cytochrome P450 (CYP119) from *Sulfolobus solfataricus*: High resolution structure and functional properties. *J. Inorg. Biochem. 91*, 491–501.

41. Kassner, R. (1972) Effects of nonpolar environments on the redox potentials of heme complexes. *Proc. Natl. Acad. Sci. U.S.A. 69*, 2263–2267.
42. Churg, A. K., and Warshel, A. (1986) Control of the redox potential of cytochrome *c* and microscopic dielectric effects in proteins. *Biochemistry 25*, 1675–1681.
43. Varadarajan, R., Zewert, T. E., Gray, H. B., and Boxer, S. G. (1989) Effects of buried ionizable amino acids on the reduction potential of recombinant myoglobin. *Science 243*, 69–72.
44. Varadarajan, R., Lambright, D. G., and Boxer, S. G. (1989) Electrostatic interactions in wild-type and mutant recombinant human myoglobins. *Biochemistry 28*, 3771–3781.
45. Caffrey, M. S., Daldal, F., Holden, H. M., and Cusanovich, M. A. (1991) Importance of a conserved hydrogen-bonding network in cytochromes *c* to their redox potentials and stabilities. *Biochemistry 30*, 4119–4125.
46. Walker, F. A., Emrick, D., Rivera, J. E., Hanquet, B. J., and Buttlaire, D. H. (1988) Effect of heme orientation on the reduction potential of cytochrome b_5. *J. Am. Chem. Soc. 110*, 6234–6240.
47. Jentzen, W., Simpson, M. C., Hobbs, J. D., Song, X., Ema, T., Nelson, N. Y., Medforth, C. J., Smith, K. M., Veyrat, M., Mazzanti, M., Ramasseul, R., Marchon, J.-C., Takeuchi, T., Goddard, W. A., III, and Shelnutt, J. A. (1995) Ruffling in a series of nickel(I1) meso-tetra substituted porphyrins as a model for the conserved ruffling of the heme of cytochromes c. *J. Am. Chem. Soc. 117*, 11085–11097.
48. Ma, J.-G., Zhang, J., Franco, R., Jia, S.-L., Moura, I., Moura, J. J. G., Kroneck, P. M. H., and Shelnutt, J. A. (1998) The structural origin of nonplanar heme distortions in tetraheme ferricytochromes c3. *Biochemistry 37*, 12431–12442.
49. Adachi, S., Nagano, S., Ishimori, K., Watanabe, Y., Morishima, I., Egawa, T., Kitagawa, T., and Makino, R. (1993) Roles of proximal ligand in heme proteins: Replacement of proximal histidine of human myoglobin with cysteine and tyrosine by site-directed mutagenesis as models for P-450, chloroperoxidase, and catalase. *Biochemistry 32*, 241–252.
50. Liu, Y., Moënne-Loccoz, P., Hildebrand, D. P., Wilks, A., Loehr, T. M., Mauk, A. G., and Ortiz de Montellano, P. R. (1999) Replacement of the proximal histidine iron ligand by a cysteine or tyrosine converts heme oxygenase to an oxidase. *Biochemistry 38*, 3733–3743.
51. Reid, L. S., Taniguchi, V. T., Gray, H. B., and Mauk, A. G. (1982) Oxidation-reduction equilibrium of cytochrome b_5. *J. Am. Chem. Soc. 104*, 7516–7519.
52. Funk, W. D., Lo, T. P., Mauk, M. R., Brayer, G. D., MacGillivray, R. T. A., and Mauk, A. G. (1990) Mutagenic, electrochemical, and crystallographic investigation of the cytochrome b_5 oxidation-reduction equilibrium: Involvement of asparagine-57, serine-64, and heme propionate-7. *Biochemistry 29*, 5500–5508.
53. Lee, K.-B., Jun, E., La Mar, G. N., Rezzano, I. N., Pandey, R. K., Smith, K. M., Walker, F. A., and Buttlaire, D. H. (1991) Influence of heme vinyl- and carboxylate-protein contacts on structure and redox properties of bovine cytochrome b_5. *J. Am. Chem. Soc. 113*, 3576–3583.
54. Das, D. K., and Medhi, O. K. (1998) The role of heme propionate in controlling the redox potential of heme: Square wave voltammetry of protoporphyrinato IX iron(III) in aqueous surfactant micelles. *J. Inorg. Biochem. 70*, 83–90.
55. Kitagawa, T., Kyogoku, Y., Iizuka, T., and Saito, M. I. (1976) Nature of the iron-ligand bond in ferrous low spin hemoproteins studied by resonance Raman scattering. *J. Am. Chem. Soc. 98*, 5169–5173.
56. Spiro, T. G., and Burke, J. M. (1976) Protein control of porphyrin conformation. Comparison of resonance Raman spectra of heme proteins with mesoporphyrin IX analogues. *J. Am. Chem. Soc. 98*, 5482–5489.
57. Champion, P. M., Gunsalus, I. C., and Wagner, G. C. (1978) Resonance Raman investigations of cytochrome $P450_{CAM}$ from *Pseudomonas putida*. *J. Am. Chem. Soc. 100*, 3743–3751.
58. Spiro, T. G., Stong, J. D., and Stein, P. (1979) Porphyrin core expansion and doming in heme proteins. New evidence from resonance Raman spectra of six-coordinate high-spin iron(III) hemes. *J. Am. Chem. Soc. 101*, 2648–2655.
59. Wells, A. V., Li, P., and Champion, P. M. (1992) Resonance Raman investigations of *Escherichia coli*-expressed *Pseudomonas putida* cytochrome P450 and P420. *Biochemistry 31*, 4384–4393.
60. Cerda-Colón, J. F., Silfa, E., and López-Garriga, J. (1998) Unusual rocking freedom of the heme in the hydrogen sulfide-binding hemoglobin from *Lucina pectinata*. *J. Am. Chem. Soc. 120*, 9312–9317.
61. Peterson, E. S., Friedman, J. M., Chien, E. Y. T., and Sligar, S. G. (1998) Functional implications of the proximal hydrogen-bonding network in myoglobin: A resonance Raman and kinetic study of Leu89, Ser92, His97, and F-helix swap mutants. *Biochemistry 37*, 12301–12319.
62. Nagai, M., Aki, M., Li, R., Jin, Y., Sakai, H., Nagatomo, S., and Kitagawa, T. (2000) Heme structure of hemoglobin M Iwate [α87(F8)His Tyr]: A UV and visible resonance Raman study. *Biochemistry 39*, 13093–13105.
63. Hu, S., Morris, I. K., Singh, J. P., Smith, K. M., and Spiro, T. G. (1993) Complete assignment of cytochrome *c* resonance Raman spectra via enzymatic reconstitution with isotopically labeled hemes. *J. Am. Chem. Soc. 115*, 12446–12458.
64. Kalsbeck, W. A., Ghosh, A., Pandey, R. K., Smith, K. M., and Bocian, D. F. (1995) Determinants of the vinyl stretching frequency in protoporphyrins. Implications for cofactor-protein interactions in heme proteins. *J. Am. Chem. Soc. 117*, 10959–10968.
65. Hu, S., Smith, K. M., and Spiro, T. G. (1996) Assignment of protoheme resonance Raman spectrum by heme labeling in myoglobin. *J. Am. Chem. Soc. 118*, 12638–12646.
66. Smulevich, G., Hu, S., Rodgers, K. R., Goodin, D. B., Smith, K. M., and Spiro, T. G. (1996) Heme-protein interactions in cytochrome c peroxidase revealed by site-directed mutagenesis and resonance Raman spectra of isotopically labeled hemes. *Biospectroscopy 2*, 365–376.
67. Fruetel, J. A., Collins, J. R., Camper, D. L., Loew, G. H., and Ortiz de Montellano, P. R. (1992) Calculated and experimental absolute stereochemistry of the styrene and β-methylstyrene epoxides formed by cytochrome P450cam. *J. Am. Chem. Soc. 114*, 6987–6993.

BI800142V